INFECTION AND IMMUNITY, Oct. 2005, p. 6350–6362 Vol. 73, No. 10
0019-9567/05/$08.00+0 doi:10.1128/IAI.73.10.6350–6362.2005

Specific Antibody Can Prevent Fungal Biofilm Formation and This Effect Correlates with Protective Efficacy

Luis R. Martinez and Arturo Casadevall*

Department of Microbiology and Immunology, Albert Einstein College of Medicine, Bronx, New York

Received 7 March 2005/Returned for modification 16 May 2005/Accepted 13 July 2005

One of the most troublesome medical problems today is infection of prosthetic devices with organisms that form polysaccharide biofilms. This combined with increasing antimicrobial drug resistance is making many infectious diseases incurable. *Cryptococcus neoformans* is a human-pathogenic fungus that has a polysaccharide capsule and can form biofilms in prosthetic medical devices. We developed a system to study cryptococcal biofilm formation in vitro and studied the effect of antibody to the *C. neoformans* capsular polysaccharide on this process. *C. neoformans* biofilm formation was dependent on the presence of a polysaccharide capsule and correlated with the ability of capsular polysaccharide to bind the polystyrene solid support. Protective antibodies prevented biofilm formation whereas nonprotective antibodies were not effective. The mechanism of antibody action involved interference with capsular polysaccharide release from the fungal cell. In contrast, lactoferrin, an effector molecule of innate immune mechanisms, was unable to prevent fungal biofilm formation despite its efficacy against bacterial biofilms. Our results suggest a new role of adaptive humoral immunity whereby some antibodies can inhibit biofilm formation by encapsulated organisms. Vaccines that elicit antibody responses to capsular antigens and/or passive transfer of antibodies to microbial polysaccharides may be useful in preventing biofilm formation.

Biofilms are dynamic communities of microorganisms tenaciously attached to biological and nonbiological surfaces that are enclosed in an exopolymeric matrix (9, 15). Biofilm formation represents the most common mode of growth of microorganisms in nature, a state that presumably allows microbial cells to both survive hostile environments and disperse to colonize new niches (15). During mammalian infection microbial biofilms are more resistant to host immune mechanisms and drug therapy and constitute a formidable problem in clinical practice.

Administration of broad-spectrum antibiotics, corticosteroids, invasive medical procedures, and the AIDS epidemic are each associated with a dramatically increased incidence of invasive fungal diseases (37). *Cryptococcus neoformans* is an encapsulated yeast-like fungus that is a relatively frequent cause of meningoencephalitis in immunocompromised patients and also occasionally causes disease in apparently healthy individuals (25). This fungus has a polysaccharide capsule composed primarily of glucuronoxylomannan (GXM) that is a major contributor to *C. neoformans* virulence, since nonencapsulated strains are not pathogenic (40).

Studies of antibody-mediated protection against *C. neoformans* have provided insight into the complexity of antibody-mediated protective mechanisms (4). Antibodies to the polysaccharide capsule can enhance survival (10), promote phagocytosis (29), affect complement activation (19), alter cytokine expression in vivo (11), clear serum polysaccharide antigen (14), enhance antigen presentation (38), and modulate expression of immunologically important molecules (26). In addition, we recently demonstrated that specific antibody could inhibit GXM release from cells, possibly by cross-linking GXM molecules in the capsule (22). Since *C. neoformans* can form biofilms on medical devices that presumably contain polysaccharide components (41), this finding raised the intriguing possibility that antibody to GXM would also interfere with cryptococcal biofilm formation. However, biofilm formation for *C. neoformans* has not been investigated in vitro and there was no information available on the dynamics of this process. The objective of this study was to define conditions for *C. neoformans* biofilm growth phases, to investigate the effect of monoclonal antibodies (MAbs) on biofilm formation, and to compare the roles of innate and adaptive immune molecules in affecting *C. neoformans* biofilm formation.

MATERIALS AND METHODS

Fungi. *C. neoformans* strains 24067 and B3501 (serotype D) were acquired from the American Type Culture Collection (Manassas, Va.). *C. neoformans* H99 (serotype A) was obtained from John Perfect (Durham, NC). *C. neoformans* var. *gattii* strain I23 was acquired from Uma Banarjee (New Delhi, India). The *cap59* gene deletion mutant (C536) and its complemented strain (C538) of *C. neoformans* B3501 were acquired from K. J. Kwon-Chung (Bethesda, MD). *Candida albicans* JC5314 and *Saccharomyces cerevisiae* were obtained from Mahmoud Ghannoum (Cleveland, OH) and Lorraine Marsh (Bronx, NY), respectively.

MAbs. MAbs 18B7 (immunoglobulin G1 [IgG1]), 12A1 (IgM), 13F1 (IgM), and 21D2 (IgM) each bind to GXM and have been described previously (2, 3, 5, 28). The murine IgG1 MAbs 3671 and 5C11 were used as isotype-matched controls having specificity for phenylarsonate and arabinomannan, respectively (13, 34). MAbs 3671 and 5C11 do not bind to *C. neoformans* polysaccharide and were used as isotype-matched irrelevant controls. MAbs 18B7 and 3671 were purified by protein G affinity chromatography (Pierce, Rockford, IL). MAbs 12A1, 13F1, 21D2, and 5C11 were purified by fast-performance liquid chromatography using a Sephacryl high-resolution gel filtration column (Pharmacia Biotech, Piscataway, NJ). Antibody concentration was determined by enzyme-linked immunosorbent assay (ELISA) relative to isotype-matched standards.

Biofilm formation. *C. neoformans* was grown in Sabouraud dextrose broth (Difco Laboratories, Detroit, Mich.) for 24 h at 30°C in a rotary shaker at 150 rpm (to early stationary phase). Cells were then collected by centrifugation,

* Corresponding author. Mailing address: Department of Medicine, Albert Einstein College of Medicine, 1300 Morris Park Ave, Bronx, NY 10461. Phone: (718) 430-2215. Fax: (718) 430-8968. E-mail: casadeva@aecom.yu.edu.

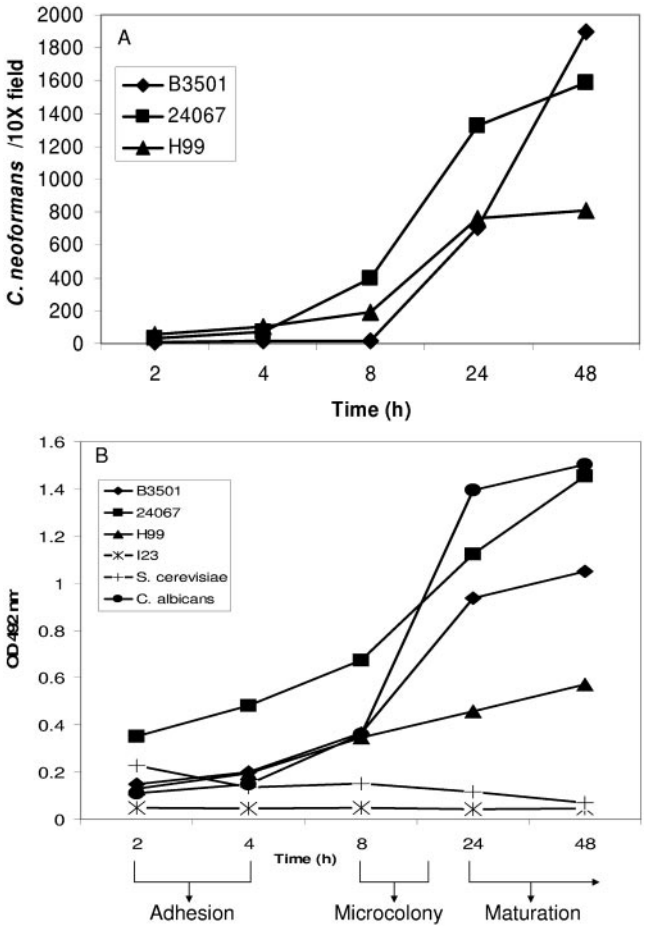

FIG. 1. A. *C. neoformans* forms biofilm in vitro. Kinetics of *C. neoformans* biofilm formation was determined by cell counts. Results are representative of two experiments. B. The kinetics of *C. neoformans* biofilm formation was compared to that of other fungi, and fungal mass was determined by XTT reduction assay. The points denote the average measurements. This experiment was done several times with similar results.

washed twice with phosphate-buffered saline (PBS), counted using a hemacytometer, and suspended at 10^7 cells per ml in minimal medium (20 mg/ml thiamine, 30 mM glucose, 26 mM glycine, 20 mM $MgSO_4 \cdot 7H_2O$, and 58.8 mM KH_2PO_4). For each strain, 100 μl of the suspension was added into individual wells of polystyrene 96-well plates (Fisher, MA) and incubated at 37°C. Biofilms were formed over a series of time intervals (2, 4, 6, 8, 24, and 48 h). Three wells in the absence of *C. neoformans* cells were utilized as controls. Following the adhesion stage, the wells containing *C. neoformans* biofilms were washed three times with 0.05% Tween 20 in Tris-buffered saline (TBS) to remove nonadhered cryptococcal cells using a microtiter plate washer (Skan Washer 400; Molecular Devices, VA). All assays were carried out in triplicate.

Quantitation of biofilm. Measurement of *C. neoformans* biofilm formation was done by counting attached cells and assessing the metabolic activity of the attached cells with the 2,3-bis(2-methoxy-4-nitro-5-sulfophenyl)-5-[(phenylamino)carbonyl]-2H-tetrazolium hydroxide (XTT) reduction assay (24).

(i) Cell counts. Biofilm formation was determined by cell counts using a PhotoZoom inverted light microscope (Cambridge Instrument, MA). The number of cryptococcal cells attached to the bottom of each well was averaged per 40-power field. This assay was done in triplicate.

(ii) XTT reduction assay. For *C. neoformans* strains, 50 μl of XTT salt solution (1 mg/ml in PBS) and 4 μl of menadione solution (1 mM in acetone; Sigma) were added to each well. Microtiter plates were incubated at 37°C for 5 h. Mitochondrial dehydrogenases in live cells reduce XTT tetrazolium salt to XTT formazan, resulting in a colorimetric change, which was measured in a microtiter reader at 492 nm. Microtiter wells containing heat-killed *C. neoformans* or only minimal medium but no *C. neoformans* cells were used as negative controls.

***C. neoformans* capsular polysaccharide isolation.** *C. neoformans* was grown in Sabouraud dextrose broth for 7 days at 30°C in a rotary shaker at 150 rpm. The supernatant was collected and filtered through a 0.45-μm membrane. Then, $NaCH_3CO_2$ was slowly added to produce a 10% weight (per volume) solution and the pH was adjusted to 7.0. *C. neoformans* capsular polysaccharide was precipitated by adding 2.5 volumes of 95 to 100% ethanol and incubated at room temperature or 4°C. Afterwards the supernatant was discarded and the polysaccharide was dissolved in distilled H_2O. Finally, the concentration of polysaccharide was measured by the phenol-sulfuric acid method.

***C. neoformans* capsular polysaccharide binding assay.** *C. neoformans* GXM was serially diluted on the plate and allowed to attach to the bottom of the wells for 2 h. Microtiter polystyrene plates were blocked with 1% bovine serum albumin (BSA) in phosphate-buffered saline to prevent non-antibody-specific binding and incubated for 1 h. Next, the IgG1 GXM binding MAb 18B7 (2 μg/ml) was added and the plate was incubated for 1 h. The ELISA was completed by adding, in successive steps, 1 μg of alkaline phosphatase-labeled goat anti-mouse IgG1/ml and 50 μl of *p*-nitrophenyl phosphate (5 mg/ml) in substrate buffer. Finally, the amount of GXM bound to the bottom of the plate was measured using a microtiter reader at 405 nm. Between every step, the wells were washed with 0.05% Tween 20 in Tris-buffered saline. All incubations were done at 37°C for 1 to 2 h or at 4°C overnight.

Effect of MAb to *C. neoformans* GXM during biofilm formation. To prevent nonspecific antibody binding, microtiter polystyrene plates were blocked with 200 μl of 1% BSA in PBS and incubated for 1 h at 37°C. Following incubation, the wells were washed three times with 0.05% Tween 20 in TBS using a microtiter plate washer. To evaluate the effect of antibody on biofilm formation, *C. neoformans* cells were grown in minimal medium in the presence or absence of GXM binding MAb 18B7, 12A1, 13F1, or 21D2 or irrelevant control MAbs 3671 and 5C11 (50 and 100 μg/ml) for 24 h at 37°C. *C. neoformans* cells and MAbs were mixed for 1 min using a microtiter plate reader mixer to ensure uniform distribution. Biofilm formation was quantified by XTT reduction assay as described above.

ELISA spot. (i) *C. neoformans* capsular polysaccharide release as a function of time. *C. neoformans* strains were grown in Sabouraud dextrose broth for 24 h at 30°C in a rotary shaker at 150 rpm (to early stationary phase). Cells were then collected by centrifugation, washed twice with PBS, counted using a hemacytometer, and suspended at 10^4 cells per ml in minimal medium. For each strain, 100 μl of the suspension was added into individual wells of polystyrene 96-well plates and incubated at 37°C. *C. neoformans* cells were allowed to adhere to the bottom of the wells over a series of time intervals (30 min and 1, 2, and 3 h). Following the adhesion stage, the wells containing *C. neoformans* biofilms were washed three times with 0.05% Tween 20 in TBS to remove nonadhered cryptococcal cells using a microtiter plate washer. All assays were carried out in five wells per strain. The wells were then blocked for nonspecific binding by adding 200 μl of 1% BSA in PBS. Next, 2 μg/ml of GXM binding MAb 18B7 in PBS (1% BSA) was added. Then, 1 μg of biotin-labeled goat anti-mouse IgG1/ml was added. Between every step, the wells were washed with 0.05% Tween 20 in TBS. All incubations were done at 37 or 4°C overnight. After the biotinylated MAb step, a 50-μl volume of 1 mg of bromo-4-chloro-3-indolyl phosphate (BCIP; Amresco, Solon, OH) per ml diluted in AMP buffer (95.8 ml of 2-amino-2-methyl-1-propanol, 0.1 ml of Triton X-405, 0.2 g of $MgCl_2 \cdot 6H_2O$ in 800 ml of double-distilled water [pH 8.6]) (Sigma Chemical Co.) was added. After 1 h the wells were washed five times with distilled water and air dried.

(ii) Effect of GXM-specific MAb 18B7 in preventing *C. neoformans* GXM release. For each *C. neoformans* strain, 100 μl of a 10^4-cell/ml suspension was added into individual wells of polystyrene 96-well plates as described above and then incubated in minimal medium in the presence or absence of GXM binding MAb 18B7 or irrelevant control MAb 3671 (50 and 100 μg/ml) for 2 h at 37°C. Following the incubation, the wells containing *C. neoformans* biofilms were washed three times with 0.05% Tween 20 in TBS to remove nonadhered cryptococcal cells using a microtiter plate washer. All assays were carried out in five wells per sample. The wells were then blocked for nonspecific binding by adding 200 μl of 1% BSA in PBS. Next, 2 μg/ml of an IgM GXM binding MAb 2D10 in PBS (1% BSA) was added. Then, 1 μg of biotin-labeled goat anti-mouse IgM/ml was added. Between every step, the wells were washed with 0.05% Tween 20 in TBS. All incubations were done at 37 or 4°C overnight. After the biotinylated MAb, a 50-μl volume of 1 mg of BCIP per ml diluted in AMP buffer was added. After 1 h, the wells were washed five times with distilled water and air dried.

Effect of lactoferrin in *C. neoformans* biofilm formation. *C. neoformans* cells were grown in minimal medium in the presence (10, 25, 50, or 100 μg/ml) or

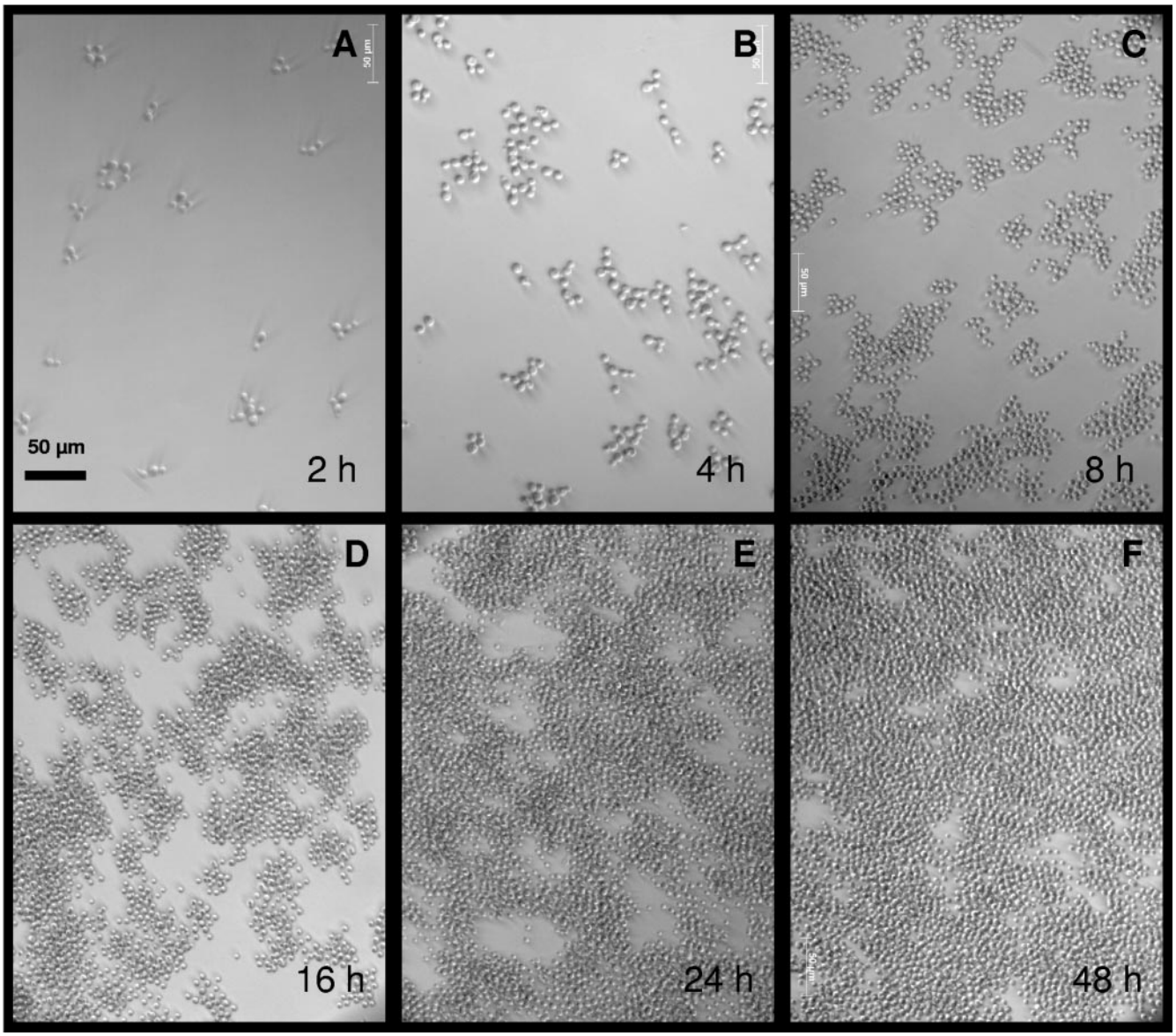

FIG. 2. Light microscopy images of *C. neoformans* B3501 biofilms after forceful washing using a microtiter plate washer. A and B. Adhesion phase (2 to 4 h). The cryptococcal cells adhere to the bottom of the wells. At this stage the biofilm consists of cells undergoing budding or fungal growth in a monolayer fashion. C and D. Intermediate phase (8 to 16 h). After attachment of the cryptococcal cells to the polystyrene plate, fungal growth involves microcolony formation consisting of cells grouped in clusters. E and F. Maturation phase (24 to 48 h). A dense network of yeast cells bound to each other is formed by a combination of capsular polysaccharide fibers and extracellular material, creating a tenacious layer consisting of cells enmeshed in polysaccharide matrix. At this point the thickness of the biofilm consists of several layers of cells. Pictures were taken using a 20-power field. The scale bar applies to all panels.

absence of lactoferrin for 24 h at 37°C in a microtiter plate. Biofilm formation was quantified by XTT reduction assay as described above.

Light microscopy. Microscopic examinations of biofilms formed in microtiter plates were performed with light microscopy using an Axiovert 200 M inverted microscope (Carl Zeiss MicroImaging, NY).

Scanning electron microscopy (SEM). *C. neoformans* biofilms were grown on glass coverslips in six-well microtiter plates with minimal medium for 48 h. Then, coverslips with biofilms were washed three times with PBS and transferred to another six-well microtiter plate containing 2.5% glutaraldehyde and incubated for 1 h at room temperature. The samples were serially dehydrated in alcohol, fixed in a critical-point drier (Samdri-790; Tousimis, Rockville, Md.), coated with gold-palladium (Desk-1; Denton Vacuum, Inc., Cherry Hill, N.J.), and viewed with a JEOL (Tokyo, Japan) JSM-6400 scanning electron microscope. Two separate sets of cultures were prepared.

Confocal microscopy (CM). *C. neoformans* biofilms were grown in 96-well microtiter plates containing minimal medium for 48 h. Wells containing mature biofilms were washed three times with PBS and incubated for 45 min at 37°C in 75 μl of PBS containing the fluorescent stains FUN-1 (10 μM) and concanavalin A (ConA)-Alexa Fluor 488 conjugate (ConA, 25 μg/ml). FUN-1 (excitation wavelength = 470 nm and emission = 590 nm) is converted to orange-red cylindrical intravacuolar structures by metabolically active cells, while ConA (excitation wavelength = 488 nm and emission = 505 nm) binds to glucose and mannose residues of cell wall and capsule polysaccharides and emits green fluorescence. Microscopic examinations of biofilms formed in microtiter plates were performed with CM using an Axiovert 200 M inverted microscope. The objective used was 40× (numerical aperture of 0.6). Depth measurements were taken at regular intervals across the width of the device. To determine the structure of the biofilms, a series of horizontal (*xy*) optical sections with a

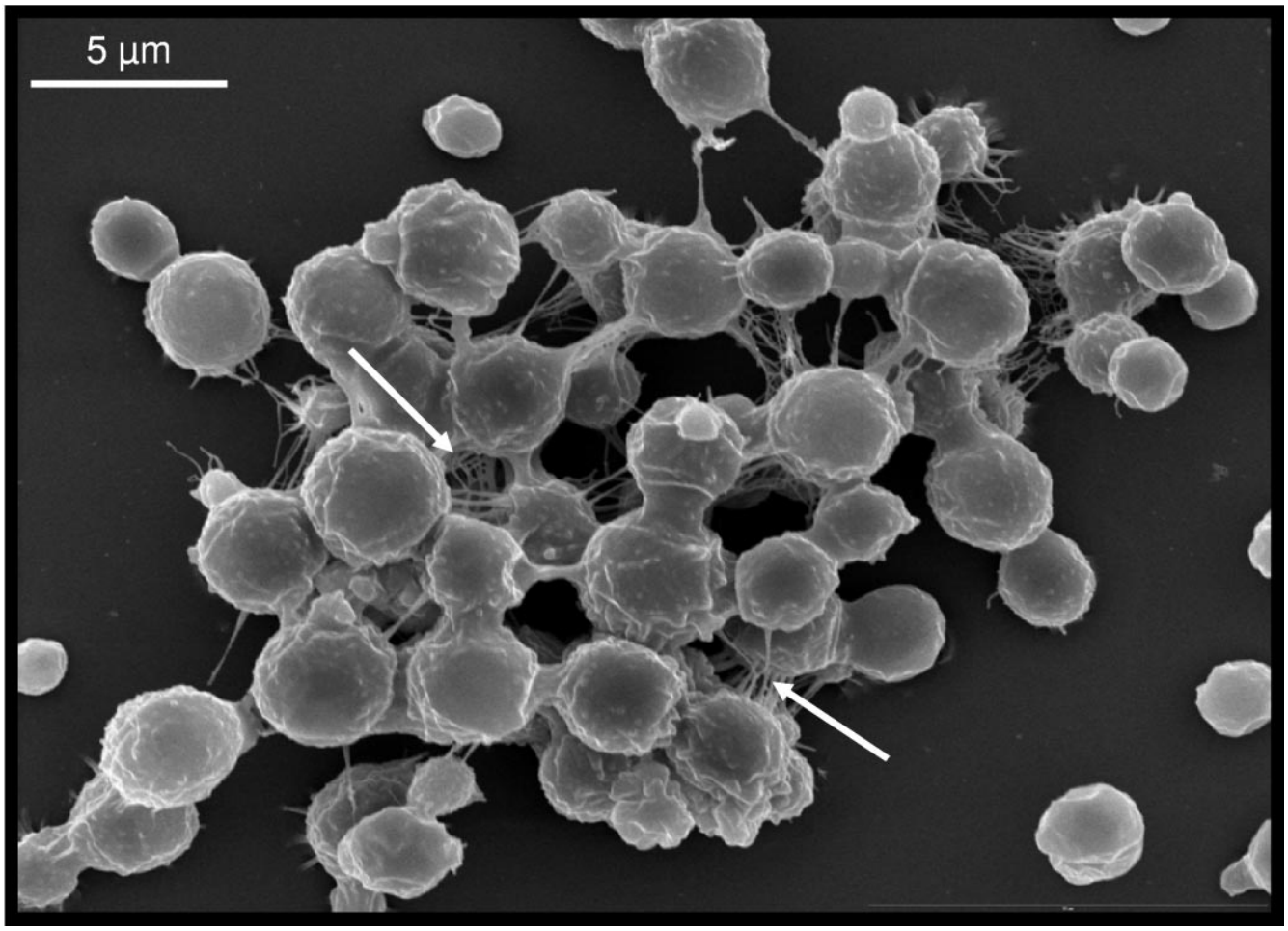

FIG. 3. Scanning electron microscopy image of mature (48-h) *C. neoformans* B3501 biofilms formed on glass coverslips revealed that cryptococcal cells are internally connected by copious amounts of polysaccharide. Arrows denote polysaccharide. Bar, 5 μm.

thickness of 1.175 μm were taken throughout the full length of the biofilm. Confocal images of green (ConA) and red (FUN-1) fluorescence were conceived simultaneously using a multichannel mode. Z-stack images and measurements were corrected utilizing Axio Vision 4.4 software-deconvolution mode (Carl Zeiss MicroImaging, NY).

Statistical analysis. All data were subjected to statistical analysis using Primer of Statistics-The Program (a software program; McGraw-Hill Co., New York, N.Y.). *P* values were calculated by analysis of variance and adjusted by the Bonferroni correction. *P* values of <0.05 were considered significant.

RESULTS

***C. neoformans* forms biofilms.** The kinetics of biofilm formation by the *C. neoformans* strains B3501, 24067, and H99 on polystyrene microtiter plates were studied using both light microscopy and the colorimetric XTT reduction assay. There was a strong correlation between cell counts and XTT reduction assay (Fig. 1A and B). Strains B3501 and 24067 were similar biofilm producers even though this process was slower for B3501. Strains B3501 and 24067 produced larger biofilms than H99. The metabolic activity of the biofilm increased over time as the cellular mass increased (Fig. 1B). Additionally, the kinetics of biofilm formation by the *C. neoformans* strains was compared to those for *Candida albicans*, a biofilm producer yeast, and *Saccharomyces cerevisiae*, a non-biofilm-forming yeast, utilizing the XTT reduction assay (Fig. 1B). The two *C. neoformans* serotype D strains were similar to each other and to *C. albicans* in their ability to form biofilms. However, the serotype A strain was significantly less effective in synthesizing a biofilm, and serotype B *C. neoformans* strain I23 was unable to form a biofilm even after the 96-h incubation period.

The cryptococcal biofilms were metabolically active during the early and intermediate stages that included the adhesion period (2 to 4 h) and microcolony formation (8 to 12 h). During the adhesion period, the cryptococcal cells became firmly attached to the plastic surface of the microtiter plate in a monolayer arrangement. The cryptococcal cells adherent to the plastic support consisted of growing cells as indicated by the presence of many budding cells (Fig. 2A and B). At the intermediate stage (8 to 16 h), the fungal population had increased significantly and consisted of yeast cells spread uniformly throughout the plastic support forming microcolonies (Fig. 2C and D). During the maturation stage (24 to 48 h), the metabolic activity of the cryptococcal cells on the biofilms remained high and steady. With increasing time the microarchitecture of *C. neoformans* biofilms became more complex due to an increasing amount of extracellular material sur-

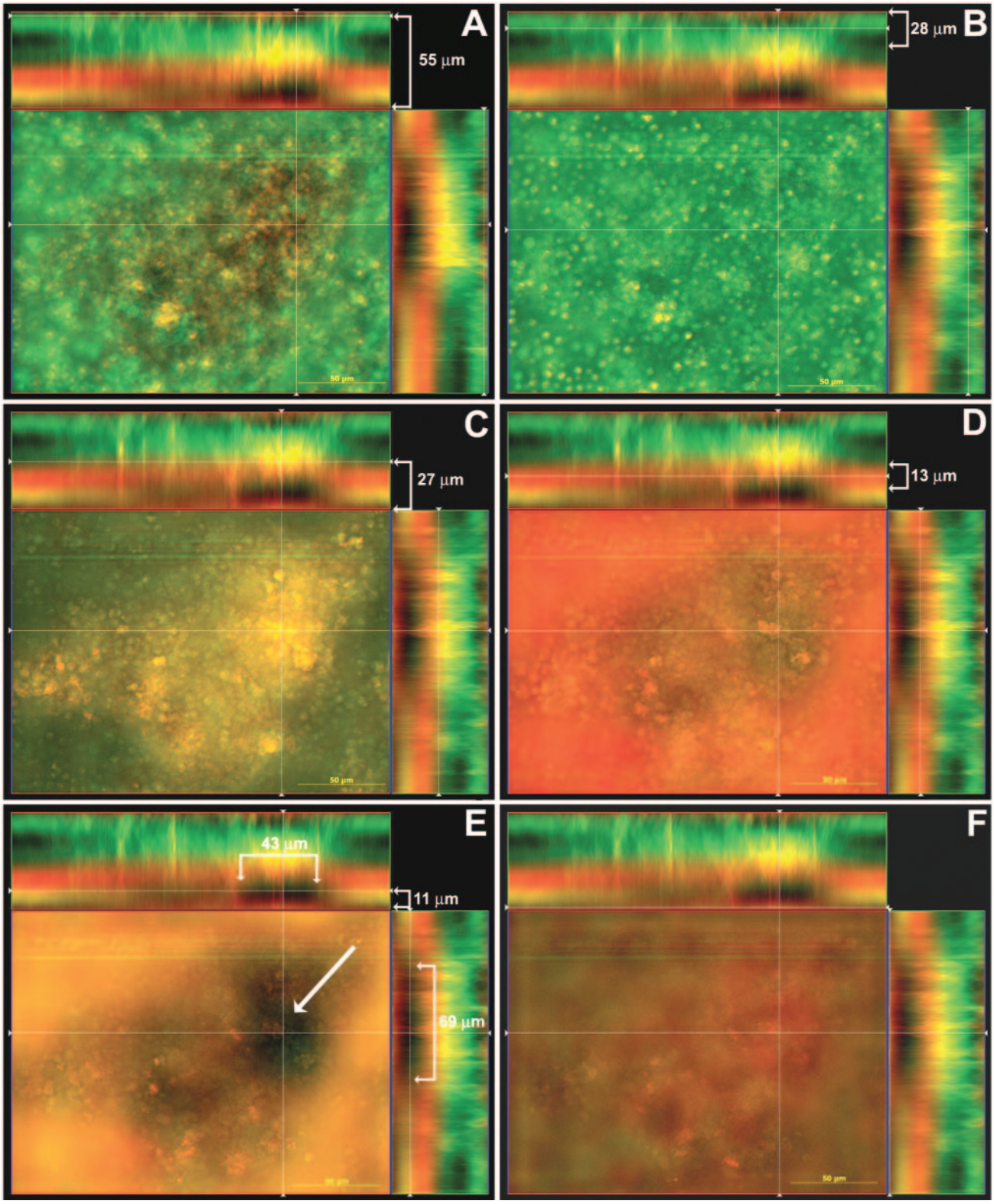

FIG. 4. CM images of a mature *C. neoformans* biofilm grown on polystyrene plates reveal a highly organized architecture. Orthogonal images of mature *C. neoformans* biofilms showed metabolically active (red, FUN-1-stained) cells embedded in the polysaccharide extracellular material (green, ConA stained). A. Mature *C. neoformans* biofilm showed a complex structure with internal regions of metabolically active cells interwoven with extracellular polysaccharide material. The thickness of a mature biofilm is approximately 55 μm. B. *C. neoformans* cells in mature biofilms were encased in exopolymeric matrix (green stained) and appeared to be approximately 28 μm thick. C. Interface of mature biofilm that separates the locations of highly metabolically active yeast cells and exopolymeric matrix. The thickness is approximately 27 μm from its starting point to the bottom of the biofilm. D. Fluorescence red-stained region within biofilm revealed the areas where most metabolically active cryptococcal cells

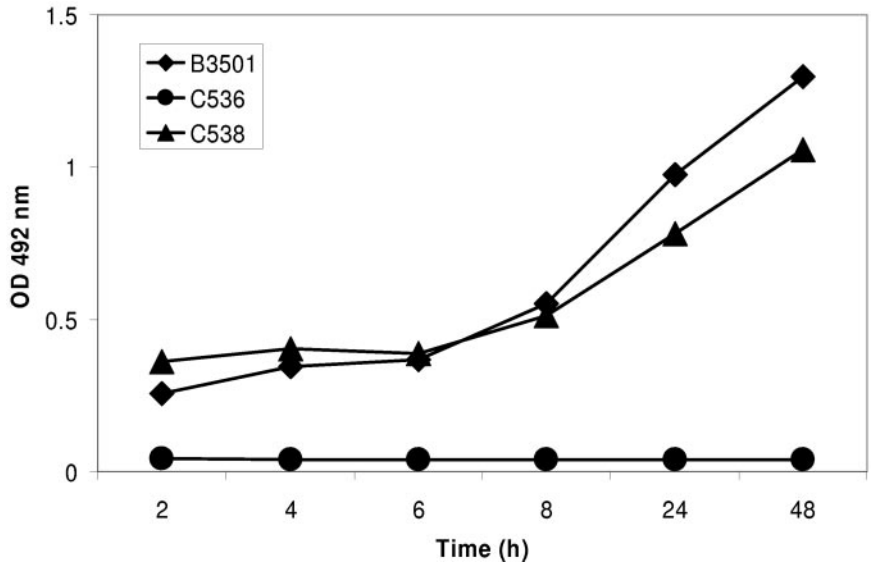

FIG. 5. *C. neoformans* polysaccharide capsule is an essential structural component of the biofilms. The kinetics of *C. neoformans* B3501 biofilm formation was compared with those of its capsule mutant (C536) and complemented strains (C538). This experiment was done twice with similar results.

rounding the cells and producing compact structures that tenaciously adhered to the plastic support (Fig. 2E and F).

SEM visualization of *C. neoformans* biofilms. Biofilm formation by *C. neoformans* on glass coverslips was monitored by SEM (Fig. 3). The fixation and dehydration steps required for SEM appeared to alter the architecture of *C. neoformans* biofilms. Nevertheless, SEM images can provide valuable insight into the structural organization of biofilms. Even though no exopolymeric matrix was seen enclosing the fungal cells, mature *C. neoformans* biofilms consisted of a dense group of cells internally connected with polysaccharide material. In contrast to many other microorganisms that form biofilms, *C. neoformans* cells strongly attached to glass and formed biofilm.

Architecture of *C. neoformans* biofilms. *C. neoformans* biofilm formation was investigated using CM because this technique preserves the structural integrity of biofilms. *C. neoformans* biofilm reconstruction was done by the compilation of a series of individual *xy* sections taken across the *z* axis. Intense green fluorescence resulting from ConA binding to polysaccharides outlined the cell walls of the yeast, while the red color due to FUN-1 staining localized in dense aggregates in the cytoplasm of metabolically active cells. Thus, areas of red fluorescence represent metabolically active cells and green fluorescence indicates cell wall-like polysaccharides, while yellow areas represent dual staining. Black areas presumably represent empty spaces that may be channels in the biofilm. In Fig. 4, orthogonal images of a mature *C. neoformans* biofilm in polystyrene 96-well plates were analyzed to determine biofilm thickness and architecture. Vertical (*xz*) sectioning (side view) of three-dimensional reconstructed images showed that mature *C. neoformans* biofilms consisted of a highly organized architecture (~55-μm-thick biofilm) with thin areas of metabolically active cells interwoven with extracellular polysaccharide material (Fig. 4A). Individual fungal cells were undistinguishable due to the aggregation of exopolymeric material (Fig. 4A). *C. neoformans* cells in mature biofilms were encased in an exopolymeric matrix (~28 μm thick) which appeared as green fluorescence (Fig. 4B). Individual yeast cells covered by polysaccharide could be distinguished in the top image (Fig. 4B). Metabolically active yeast cells were located in a boundary layer as shown in Fig. 4C. The thickness of the biofilm interface was ~27 μm. A top view showed yellow-brownish-stained yeasts. However, the region in which most of the metabolically active cryptococcal cells were located was ~13 μm thick (Fig. 4D). As described for other organisms, channels were apparent in the biofilm structure (Fig. 4E). One channel of ~69 μm in length and ~43 μm in width appeared to be a structural component of the imaged section of this *C. neoformans* biofilm. The side view of the biofilm showed the presence of dual-stained yeast neighboring the channel. The top view of the image showed the location of the channel. Finally, the bottom of a *C. neoformans* biofilm consisted of mainly dual-stained cryptococcal cells and scattered porosity (Fig. 4F).

***C. neoformans* polysaccharide capsule is important for biofilm formation.** We investigated the role of the capsule in cryptococcal biofilm formation by comparing the biofilm-forming properties of acapsular and encapsulated strains (Fig. 5). These studies used the acapsular *cap59* gene deletion mutant (C536), its encapsulated complemented strain (C538), and the wild-type parent encapsulated strain B3501. The *C. neofor-*

are located. This region is approximately 13 μm thick. E. A flowing channel appears as a dark patch in the *C. neoformans* biofilm. This channel is approximately 69 μm in length and 43 μm in width and is mainly surrounded by dual-stained (yellow) yeast cells. Arrows denote the location of the channel in the mature cryptococcal biofilm. F. The bottom of a *C. neoformans* biofilm consisted of mainly dual-stained cryptococcal cells and scattered porous regions. Pictures were taken using a 40-power field. Bar, 50 μm.

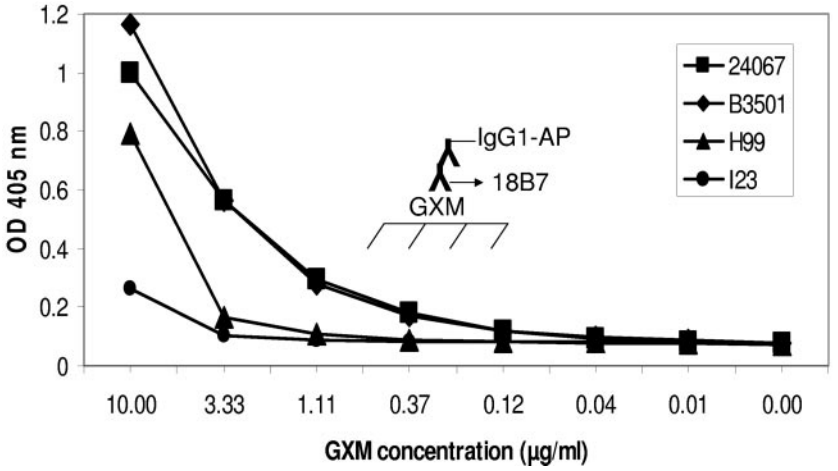

FIG. 6. Binding of serotype A, B, or D capsular polysaccharide to the plastic surface of a microtiter plate. Serotype D strain capsular polysaccharide of *C. neoformans* attached best to the polystyrene microtiter plate. The inset diagram indicates the ELISA configuration used to detect the polysaccharide bound to the bottom of the plate. AP, alkaline phosphatase.

mans cap59 mutant manifested no evidence of biofilm formation after 48 h by XTT assay. In contrast, *C. neoformans* B3501 and the complemented strain C538 manifested similar biofilm-forming capacities. This result implicates the polysaccharide capsule as an important structural component for biofilm formation. We evaluated whether the acapsular strain C536 could recover the capacity for biofilm formation when grown in the presence of exogenous GXM (0.5 mg/ml) but found no evidence of a biofilm (data not shown).

***C. neoformans* strain biofilm formation correlates with the ability of GXM to bind polystyrene.** Since purified GXM from *C. neoformans* strains differing in serotype is known to differ in its ability to bind polystyrene (39), we investigated whether there was a correlation between GXM binding to plastic and strain biofilm formation. Total capsular polysaccharide of *C. neoformans* serotypes A, B, and D was isolated and added to polystyrene plates, and binding was detected with MAbs. GXM from *C. neoformans* serotype D strains B3501 and 24067 adhered better to the polystyrene material than serotypes A (H99) and B (var. *gattii*) strains, respectively (Fig. 6). *C. neoformans* H99 showed an intermediate binding to the experimental plastic surface whereas *C. neoformans* I23 did not show binding to the bottom of the wells. Hence, the relative ability of GXM to bind polystyrene correlated with the strain biofilm-forming capacity in that support.

ELISA spot. The ELISA spot was used to investigate the mechanism of *C. neoformans* biofilm formation, and in particular the time dependence of polysaccharide release upon contact with the plastic surface. Light microscopy was used to quantify the number of cells that attached to plastic as measured by spot formation (Fig. 7B). *C. neoformans* 24067 cells produced the largest number of spots followed by H99 and B3501 strains, respectively (Fig. 7C). The number of spots observed for *C. neoformans* 24067 and H99 strains increased with time whereas for *C. neoformans* B3501 the spot number remained low and constant after a 3-h incubation period.

In addition, the surface area of the spots was measured by tracing the circumference of the whole spot left by the organism at the equatorial plane (area = πr^2) (Fig. 7D). This was done to determine the area involved in binding of GXM released by *C. neoformans* cells on the spot of attachment. Spots from *C. neoformans* serotype D strains were significantly larger than those from the H99 strain, consistent with greater binding to the plate at the site of cell-plastic contact. There was no correlation between the number of *C. neoformans* cells bound to the plate and the area of the spots left by the attached cells.

MAb to *C. neoformans* GXM prevents biofilm formation. Given the requirement for capsular polysaccharide in biofilm formation, we evaluated the effect of specific antibody in this phenomenon. *C. neoformans* B3501, 24067, and H99 strains were each grown in the absence of MAb or with 50 and 100 μg of MAb 18B7 (IgG1) or irrelevant MAb 3671 (IgG1) per ml at 37°C (Fig. 8A). *C. neoformans* B3501 and 24067 strains did not form biofilms when incubated with specific MAb. In contrast, cells of these strains grown in the absence of MAb or grown in the presence of isotype-matched control MAb 3671 formed biofilms. *C. neoformans* H99 did not produce a strong biofilm under any condition. To determine whether *C. neoformans* cells were growing similarly in the presence and in the absence of MAb, the metabolic activity of the fungal cells was measured by XTT reduction assay after 24 h by adding it directly to the medium without washing off the cells from the wells. All the strains showed equivalent metabolic activity under all the conditions, indicating that inhibition of biofilm formation by MAb occurred without antibody-mediated inhibition of growth or metabolic activity. Hence, specific antibody interfered with biofilm formation but not fungal growth.

To determine the mechanism by which GXM-specific MAb 18B7 inhibits *C. neoformans* biofilm formation, the ELISA spot assay was utilized. This assay was used to examine local release of capsular polysaccharide by attached cryptococcal cells and the role of this polysaccharide in the creation of an exopolysaccharide matrix for *C. neoformans* biofilm formation. *C. neoformans* 24067 and B3501 grown in the presence of MAb 18B7 (50 and 100 μg/ml) bound to the bottom of the polystyrene plate but did not form blue spots in comparison with cells grown in the absence of antibody or in the presence of irrelevant MAb 3671 (Fig. 8B).

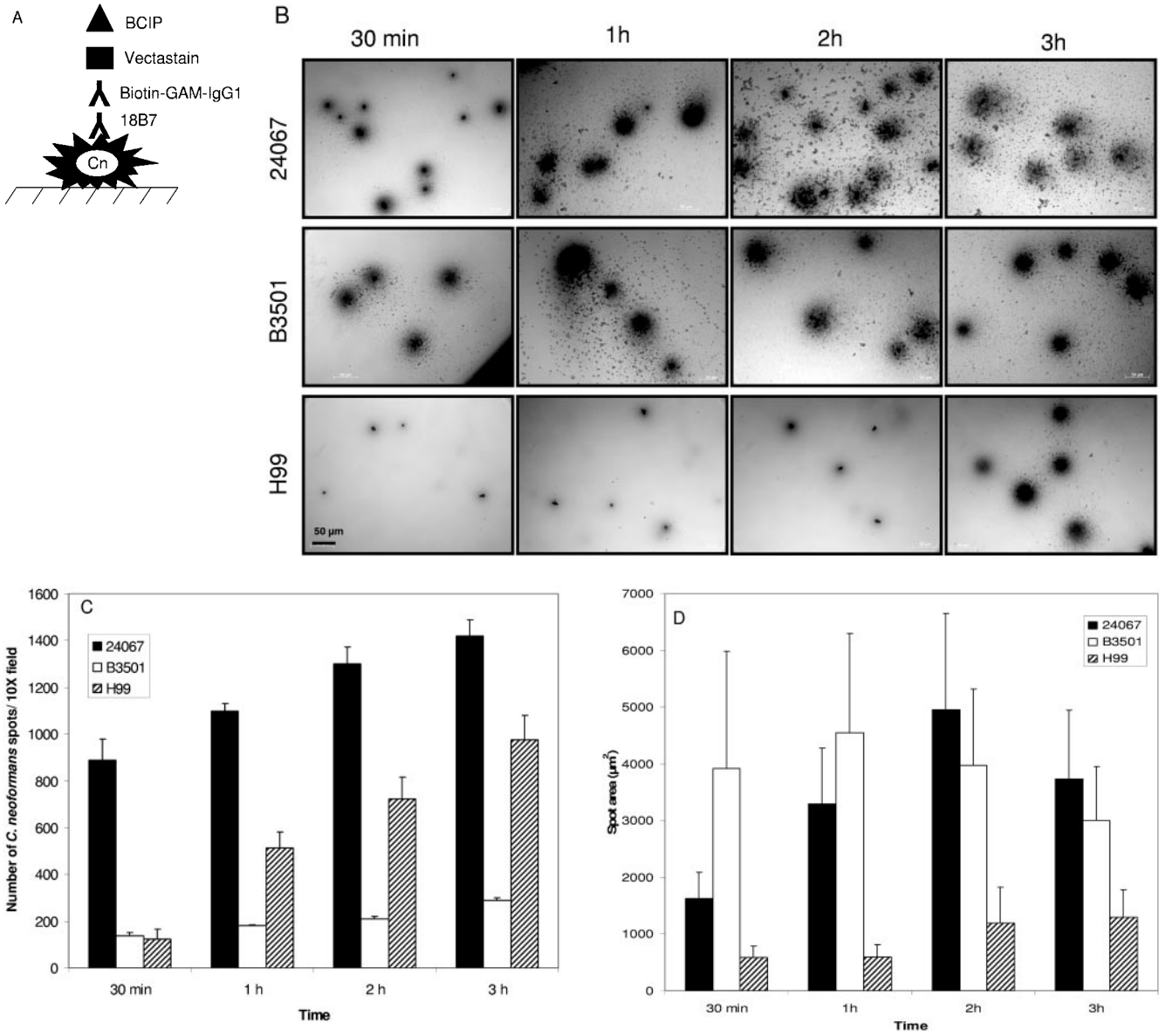

FIG. 7. A. Graphic representation of the ELISA spot configuration. The diagram indicates the antibodies (MAb 18B7 and goat anti-mouse [GAM] IgG1 conjugated to biotin) used to recognize the GXM released by *C. neoformans* (Cn) cells to the bottom of the plate. B. Light microscopic images of spots formed by *C. neoformans* strains 24067, B3501, and H99 during ELISA spot assay. Images were obtained after 30 min and 1, 2, and 3 h of incubation in polystyrene microtiter plates. Bars, 50 μm. Results are representative of two experiments. C. Spot number in microtiter wells as a function of time for three biofilm-forming strains of *C. neoformans*. Bars are the average numbers of spots in five power fields, and error bars denote standard deviations. Pictures were taken using a 20-power field. D. Spot area as a function of time for three biofilm-forming strains. GXM amount was visualized by ELISA spot assay. Bars are the averages of the areas of 20 spots per power field with the area being calculated as $= \pi r^2$. Five power fields were observed per time interval. Error bars denote standard deviations. Pictures were taken using a 20-power field.

Protective MAb to *C. neoformans* polysaccharide capsule prevents biofilm formation. To investigate whether a relationship existed between the protective efficacy of antibodies and their ability to inhibit biofilm formation, we compared biofilm formation in the presence of protective and nonprotective antibodies. MAbs 12A1 and 13F1 are IgM antibodies to GXM that differ in specificity, protective efficacy, and inhibition of capsular polysaccharide release despite using the same variable region genes and originating from the same B-cell precursor (22, 27, 31). MAb 21D2 uses the same variable gene elements as the MAb 12A1 and 13F1 pair but recognizes a different epitope and, like 13F1, is not protective. Fungal cells incubated in the presence of specific MAb 12A1 did not form biofilms (Fig. 9). In contrast, *C. neoformans* B3501 cells grown in the absence of MAb or grown in the presence of MAb 13F1, MAb 21D2, or isotype-matched control MAb 5C11 formed similar biofilms. Hence, the protective MAb 12A1 significantly reduced the ability of *C. neoformans* to form biofilms whereas the

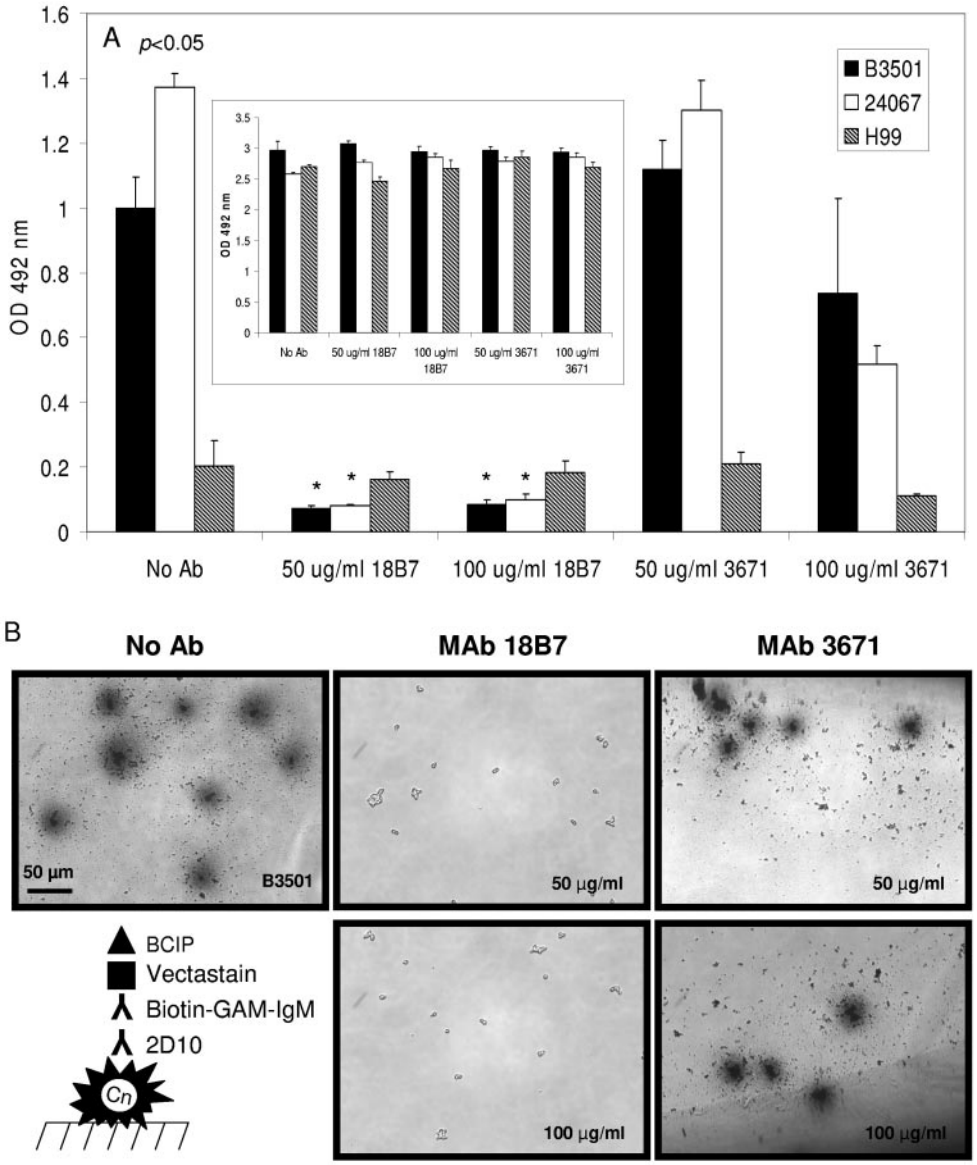

FIG. 8. A. *C. neoformans* biofilm formation is inhibited by the presence of IgG1 MAb 18B7, which binds GXM. The inset graph indicates the metabolic activity of *C. neoformans* B3501, 24067, and H99 cells grown in the presence or absence of MAb. The absence of differences indicates that specific antibody has no effect on fungal growth. Bars are the averages of three measurements, and error bars denote standard deviations. Asterisks denote *P* value significance calculated by analysis of variance and adjusted by the Bonferroni correction. B. MAb 18B7 prevents *C. neoformans* B3501 biofilm formation by interference with capsular polysaccharide release. Light microscopic images of spots formed by *C. neoformans* B3501during ELISA spot assay. Images were obtained after 2 h of incubation of fungal cells in the absence and presence of GXM binding MAb 18B7 or irrelevant antibody 3671 in a polystyrene microtiter plates. Results are representative of two experiments. Inset is a graphic representation of the ELISA spot configuration utilized. The diagram indicates the antibodies (MAb 2D10 and goat anti-mouse [GAM] IgM conjugated to biotin) used to recognize the GXM released by *C. neoformans* (Cn) cells to the bottom of the plate.

nonprotective MAbs 13F1 and 21D2 did not interfere with biofilm formation.

Lactoferrin does not prevent *C. neoformans* biofilm formation. Lactoferrin is a protein of the innate immune system that can prevent bacterial biofilm formation (36). The effect of lactoferrin on *C. neoformans* biofilm production was investigated using the XTT reduction assay. *C. neoformans* B3501, 24067, and H99 strains were grown in the absence of lactoferrin or with 10, 25, 50, or 100 μg of lactoferrin at 37°C without shaking. After 24 h, lactoferrin did not affect significantly the ability of *C. neoformans* B3501 and 24067 to form biofilms (Fig. 10). *C. neoformans* H99 did not produce a strong biofilm regardless of the presence of lactoferrin.

DISCUSSION

C. neoformans biofilm formation was inferred from the observation that cells grown in polystyrene plates formed a tenacious attachment to a plastic surface consisting of metabolically active microcolonies enmeshed in a polysaccharide-

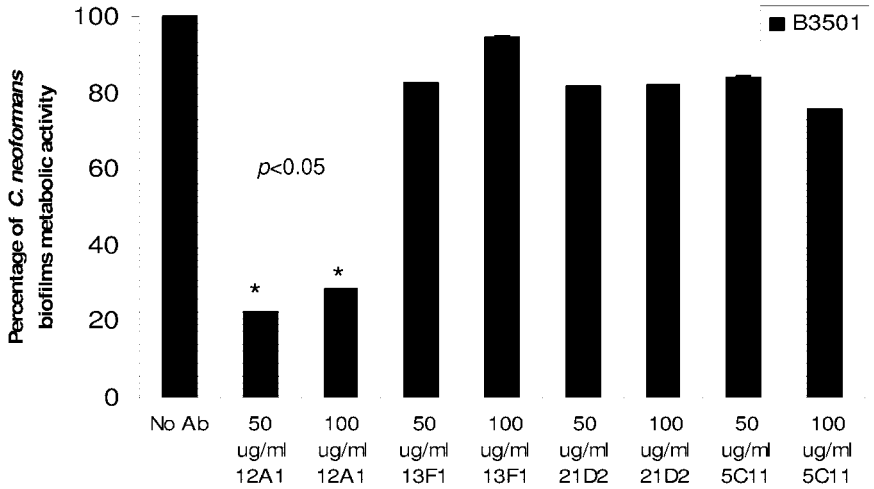

FIG. 9. Specific IgM MAb 12A1 significantly inhibits *C. neoformans* B3501 strain biofilm production. Bars are the averages of three measurements, and error bars denote standard deviations. Asterisks denote *P* value significance calculated by analysis of variance and adjusted by the Bonferroni correction. These experiments were done twice with similar results.

containing matrix. *C. neoformans* biofilm formation resembled *C. albicans* biofilm formation in that it progressed through coordinated phases such as early, intermediate, and maturation stages (6). In early growth phase, *C. neoformans* cells strongly adhered to the plastic support. For some microbes external features on the cell surface of the microorganism such as fimbriae, flagella, or capsule influence the rate and extent of attachment of microbial cells (1, 33). *C. neoformans* polysaccharide capsule may provide the yeast cells with an advantage in the attachment process. The dynamic nature of the capsule could allow *C. neoformans* cells to interact favorably with a variety of substrata and promote fungal attachment. The intermediate phase of *C. neoformans* biofilm growth is characterized by a homogeneous aggregation of yeast cells in a microcolony arrangement on the surface where a biofilm is forming. Proximity of fungal cells within the microcolony may present a formidable environment for the establishment of nutrient gradients, genetic exchange, and quorum sensing. *C. neoformans* mature biofilms consisted of a dense arrangement of yeast cells embedded within GXM and extracellular material. This structural organization and the presence of flowing channels may allow nutrient and gas exchange while providing the yeast cells with a sheltered niche for protection against environmental predators, immune cells, shear forces, and antifungal drugs. *C. neoformans* biofilm formation may also be involved in mammalian pathogenesis. In this regard it is noteworthy that changes in *C. neoformans* capsular structure have been reported during crossing of the blood-brain barrier (7) and yeast cells in brain tissue usually surrounded by extracellular polysaccharide (21).

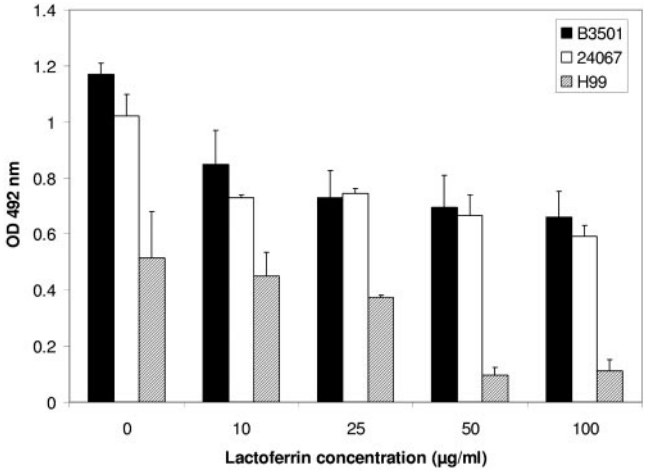

FIG. 10. *C. neoformans* biofilm formation is not inhibited by the presence of lactoferrin. Bars are the averages of three measurements, and error bars denote standard deviations. These experiments were done twice with similar results.

The studies with the acapsular *cap59* mutant C536 revealed no biofilm formation relative to the parent strain 3501 or the encapsulated complemented mutant 538. This indicated that capsular polysaccharide was necessary for biofilm formation and implied a role for capsular polysaccharide in this process. Since the *C. neoformans* capsule is composed primarily of GXM and since GXM is a constituent of the cryptococcal extracellular biofilm matrix, it is reasonable to conclude that the inability of the acapsular mutant strain C536 to form a biofilm reflects an inability to shed polysaccharide and form a matrix. Addition of exogenous polysaccharide to acapsular cell cultures was not sufficient to compensate for lack of capsular production in biofilm formation. GXM from serotype D attached best to polystyrene plates consistent with the prior reports that the relative binding ability of serotype GXM to polystyrene was D > A ≫ B and C (3). Although the molecular basis of this phenomenon has not been investigated, the ability to bind polystyrene appeared to be inversely proportional to the complexity, and degree of substitution, of the GXM triad structure. Hence, the observation that the serotype D strains made more robust biofilms combined with the serotype differences in binding polystyrene GXM and the presence of GXM in the biofilm provided a compelling case for the

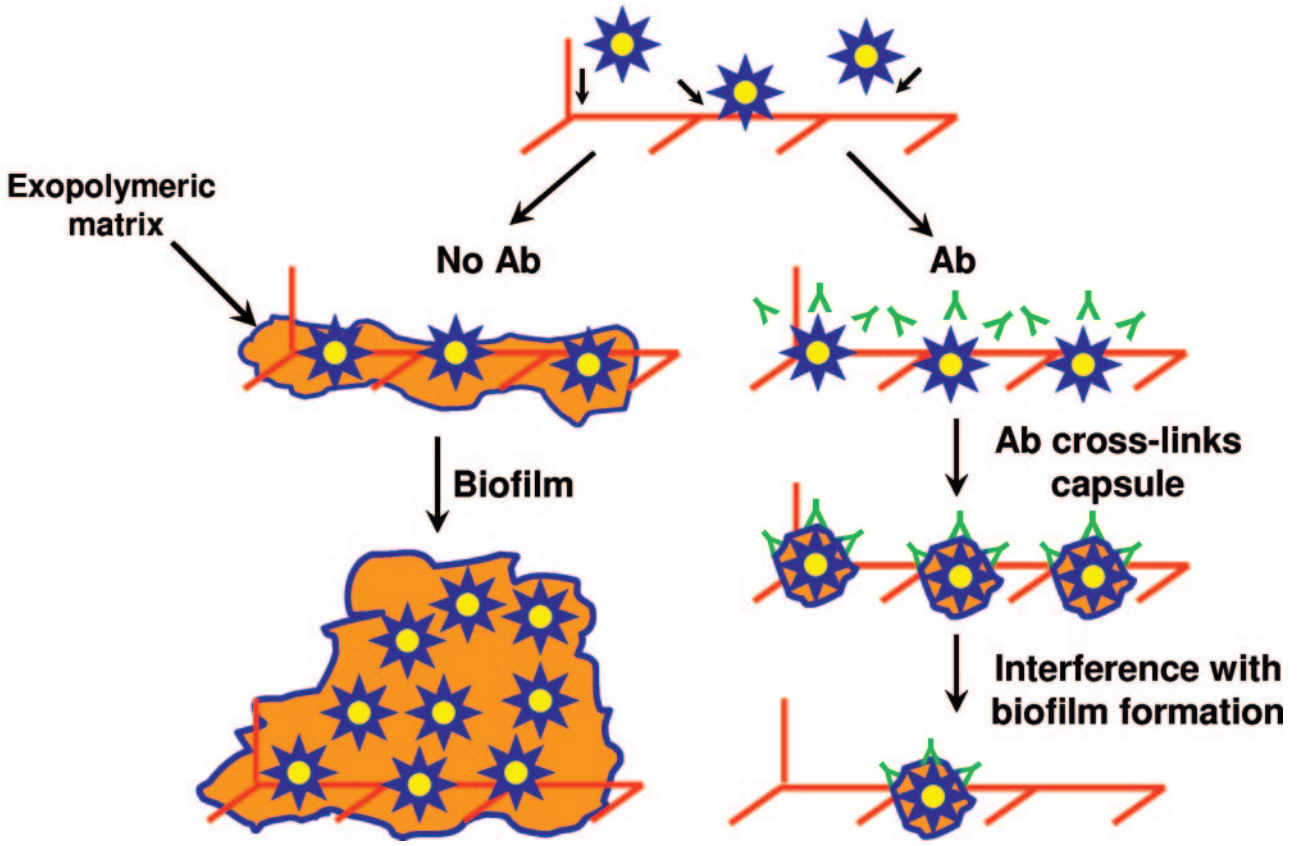

FIG. 11. Model of antibody-mediated inhibition of *C. neoformans* biofilm formation. In the absence of MAb, *C. neoformans* cells release capsular polysaccharide which is involved in attachment to the plastic surface. In the presence of a MAb specific to *C. neoformans* polysaccharide capsule the immunoglobulin prevents capsular polysaccharide release, which blocks the adhesion of the yeast cells to the surface.

importance of GXM binding as a critical event in *C. neoformans* biofilm formation.

An ELISA spot assay was used to investigate the importance of *C. neoformans* capsular polysaccharide release in biofilm formation. This assay also provided an alternate method to confirm the results obtained by XTT assay. The number and area of spots on microtiter plates were determined as a function of time using light microscopy. Biofilm formation by *C. neoformans* did not correlate with the number of yeast cells bound to the plastic support surface. For instance, serotype A strain H99 attached in larger quantities to the plastic surface of the microtiter plate but produced smaller spots than those formed by both serotype D strains. This result implies that cell adhesion was a necessary but not sufficient event for biofilm formation. In fact, we interpret the ELISA spot data as indicating the need for local release of capsular polysaccharide by attached cells and the binding of shed polysaccharide to the plastic surface to create an exopolysaccharide matrix. We surmise that cell-cell interactions are maximized in situations where both the cell and the polysaccharide bind to create a robust exopolymeric network that snares yeast cells to form a biofilm. In this regard the greater biofilm-forming capacity of serotype D cells relative to the serotype A and B cells probably reflects enhanced ability of their GXM to bind the plastic support.

Although the polysaccharide capsule of *C. neoformans* is critical for biofilm formation, this role of this structure in microbial biofilm formation can vary with the organism. For *Escherichia coli*, the presence of a capsule blocks the function of a self-recognizing protein antigen and physically interferes with biofilm formation (35). Similarly, expression of capsular polysaccharides by *Vibrio vulnificus* interferes with biofilm formation (18). However, for *Staphylococcus epidermidis* biofilm formation is associated with the production of an extracellular polysaccharide (23). The disparate effects of the capsule biofilm formation may reflect chemical properties of the polysaccharide. Consistent with this view are the findings that O acetylation of alginate contributed to biofilm formation (30) and the *C. neoformans* strain-related differences in biofilm formation.

Addition of GXM binding MAb to *C. neoformans* cultures in microtiter plates prevented biofilm formation. This function has not been previously described for specific antibodies to polysaccharides and suggests a new role for humoral immunity in defense against biofilm-forming microbes. Since an isotype-matched nonspecific antibody was not able to interfere with biofilm formation, we can exclude explanations that involve blocking of GXM attachment to the plate by competition with GXM binding sites in the polystyrene support or steric hindrance. The fact that polysaccharide is required for cryptococcal biofilm formation combined with the observation that specific antibody inhibits GXM release from encapsulated cells (7)

suggests a mechanism for antibody action. Consistent with this mechanism, we observed that the specific MAb interfered with ELISA spot formation but not attachment. A model for antibody-mediated inhibition of biofilm formation is outlined in Fig. 11. Passive antibody therapy, vaccination to induce specific antibody responses, or engineering of antibody into certain surfaces may be a useful strategy in combating biofilm-producing microbes. Moreover, we associated antibody-mediated inhibition of biofilm formation with protective antibodies, suggesting the tantalizing possibility that this effect is involved in antibody protective efficacy against *C. neoformans*.

Singh et al. have recently demonstrated that lactoferrin could prevent development of bacterial biofilms (36). However, lactoferrin did not inhibit *C. neoformans* biofilm formation, implying that this component of innate immunity was insufficient in preventing the establishment of the fungal biofilms. Bacteria obtain iron using siderophores. Lactoferrin is hypothesized to interfere with iron acquisition in bacteria. In contrast, *C. neoformans* is a soil organism with a mechanism for iron uptake that is siderophore independent (16, 17). In fact, *C. neoformans* may obtain iron by any of three mechanisms that involve extracellular reduction of Fe^{3+} to Fe^{2+} by a cell-associated ferric reductase, secretion of 3-hydroxyanthranilic acid, and melanin (32). These systems can function in parallel, and consequently it may be more difficult for the iron-limiting defense mechanism of innate immunity to block *C. neoformans* biofilm formation.

In summary, we report biofilm formation by *C. neoformans*, a phenomenon that may confer on this fungus the ability to resist predators in the environment and protect against host immune mechanisms and antifungal therapy. Our results indicated that capsular production and polysaccharide binding to plastic support are critical steps for *C. neoformans* biofilm formation. The observation that MAbs to *C. neoformans* GXM could inhibit biofilm formation indicates a new function for specific antibodies and suggests that adaptive humoral immune responses may be critically important for preventing the formation of microbial biofilms. Furthermore, the results imply a potential usefulness for antibodies in the clinical management of disease caused by biofilm-forming microbes, including cryptococcosis. In this regard, a MAb to *C. neoformans* polysaccharide is already in clinical trial evaluation (20) and vaccines that elicit antibodies to the polysaccharide exist (8, 12). Hence, either passive antibody administration or immunization may be useful in diminishing cryptococcal biofilm formation in ventricular shunts. Specific antibody may prevent biofilm formation for other microbes, and this could suggest a broad strategy for combating this troublesome medical problem.

ACKNOWLEDGMENTS

We thank Fernando Macian for allowing us the use of his inverted light microscope (Zeiss Axiovert 200 M) for these studies.

NIH awards AI033142-11, AI033774-11, and HL059842-08 supported this work.

REFERENCES

1. **Bullitt, R., and L. Makowski.** 1995. Structural polymorphism of bacterial adhesion pili. Nature **373:**164–167.
2. **Casadevall, A., W. Cleare, M. Feldmesser, A. Glatman-Freedman, D. L. Goldman, T. R. Kozel, N. Lendvai, J. Mukherjee, L. A. Pirofski, J. Rivera, A. L. Rosas, M. D. Scharff, P. Valadon, K. Westin, and Z. Zhong.** 1998. Characterization of a murine monoclonal antibody to *Cryptococcus neoformans* polysaccharide that is a candidate for human therapeutic studies. Antimicrob. Agents Chemother. **42:**1437–1446.
3. **Casadevall, A., J. Mukherjee, and M. D. Scharff.** 1992. Monoclonal antibody based ELISAs for cryptococcal polysaccharide. J. Immunol. Methods **154:** 27–35.
4. **Casadevall, A., and L. Pirofski.** 2003. Antibody-mediated regulation of cellular immunity and the inflammatory response. Trends Immunol. **24:**474–478.
5. **Casadevall, A., and M. D. Scharff.** 1991. The mouse antibody response to infection with *Cryptococcus neoformans*: VH and VL usage in polysaccharide binding antibodies. J. Exp. Med. **174:**151–160.
6. **Chandra, J., D. M. Kuhn, P. K. Mukherjee, L. L. Hoyer, T. McCormick, and M. A. Ghannoum.** 2001. Biofilm formation by the fungal pathogen *Candida albicans*: development, architecture, and drug resistance. J. Bacteriol. **183:** 5385–5394.
7. **Charlier, C., F. Chretien, M. Baudrimont, E. Mordelet, O. Lortholary, and F. Dromer.** 2005. Capsule structure changes associated with *Cryptococcus neoformans* crossing of the blood-brain barrier. Am. J. Pathol. **166:**421–432.
8. **Devi, S. J., R. Schneerson, W. Egan, T. J. Ulrich, D. Bryla, J. D. Robbins, and J. E. Bennett.** 1991. *Cryptococcus neoformans* serotype A glucuronoxylomannan-protein conjugate vaccines: synthesis, characterization, and immunogenicity. Infect. Immun. **59:**3700–3707.
9. **Donlan, R. M.** 2002. Biofilms: microbial life on surfaces. Emerg. Infect. Dis. **8:**881–890.
10. **Dromer, F., J. Charreire, A. Contrepois, C. Carbon, and P. Yeni.** 1987. Protection of mice against experimental cryptococcosis by anti-*Cryptococcus neoformans* monoclonal antibody. Infect. Immun. **55:**749–752.
11. **Feldmesser, M., A. Mednick, and A. Casadevall.** 2002. Antibody-mediated protection in murine *Cryptococcus neoformans* infection is associated with pleotrophic effects on cytokine and leukocyte responses. Infect. Immun. **70:**1571–1580.
12. **Fleuridor, R., A. Lees, and L. Pirofski.** 2001. A cryptococcal capsular polysaccharide mimotope prolongs the survival of mice with *Cryptococcus neoformans* infection. J. Immunol. **166:**1087–1096.
13. **Glatman-Freedman, A., J. M. Martin, P. F. Riska, B. R. Bloom, and A. Casadevall.** 1996. Monoclonal antibodies to surface antigens of *Mycobacterium tuberculosis* and their use in a modified enzyme-linked immunosorbent spot assay for detection of mycobacteria. J. Clin. Microbiol. **34:**2795–2802.
14. **Goldman, D. L., S. C. Lee, and A. Casadevall.** 1995. Tissue localization of *Cryptococcus neoformans* glucuronoxylomannan in the presence and absence of specific antibody. Infect. Immun. **63:**3448–3453.
15. **Hall-Stoodley, L., J. W. Costerton, and P. Stoodley.** 2004. Bacterial biofilms: from the natural environment to infectious diseases. Nat. Rev. Microbiol. **2:**95–108.
16. **Jacobson, E. S., and M. J. Petro.** 1987. Extracellular iron chelation in *Cryptococcus neoformans*. J. Med. Vet. Mycol. **25:**415–418.
17. **Jacobson, E. S., and S. E. Vartivarian.** 1992. Iron assimilation in *Cryptococcus neoformans*. J. Med. Vet. Mycol. **30:**443–450.
18. **Joseph, L. A., and A. C. Wright.** 2004. Expression of *Vibrio vulnificus* capsular polysaccharide inhibits biofilm formation. J. Bacteriol. **186:**889–893.
19. **Kozel, T. R., B. C. deJong, M. M. Grinsell, R. S. MacGill, and K. K. Wall.** 1998. Characterization of anticapsular monoclonal antibodies that regulate activation of the complement system by the *Cryptococcus neoformans* capsule. Infect. Immun. **66:**1538–1546.
20. **Larsen, R. A., P. G. Pappas, J. Perfect, J. A. Aberg, A. Casadevall, G. A. Cloud, R. James, S. Filler, and W. E. Dismukes.** 2005. Phase I evaluation of the safety and pharmacokinetics of murine-derived anticryptococcal antibody 18B7 in subjects with treated cryptococcal meningitis. Antimicrob. Agents Chemother. **49:**952–958.
21. **Lee, S. C., A. Casadevall, and D. W. Dickson.** 1996. Immunohistochemical localization of capsular polysaccharide antigen in the central nervous system cells in cryptococcal meningoencephalitis. Am. J. Pathol. **148:**1267–1274.
22. **Martinez, L. R., D. Moussai, and A. Casadevall.** 2004. Antibody to *Cryptococcus neoformans* glucuronoxylomannan inhibits the release of capsular antigen. Infect. Immun. **72:**3674–3679.
23. **McKenney, D., J. Hubner, E. Muller, Y. Wang, D. A. Goldmann, and G. B. Pier.** 1998. The *ica* locus of *Staphylococcus epidermidis* encodes production of the capsular polysaccharide/adhesin. Infect. Immun. **66:**4711–4720.
24. **Meshulam, T., S. M. Levitz, L. Christin, and R. D. Diamond.** 1995. A simplified new assay for assessment of fungal cell damage with the tetrazolium dye, (2,3)-bis-(2-methoxy-4-nitro-5-sulphenyl)-(2H)-tetrazolium-5-carboxanilide (XTT). J. Infect. Dis. **172:**1153–1156.
25. **Mitchell, T. G., and J. R. Perfect.** 1995. Cryptococcosis in the era of AIDS—100 years after the discovery of *Cryptococcus neoformans*. Clin. Microbiol. Rev. **8:**515–548.
26. **Monari, C., F. Bistoni, A. Casadevall, E. Pericolini, D. Pietrella, T. R. Kozel, and A. Vecchiarelli.** 2005. Glucuronoxylomannan, a microbial compound, regulates expression of costimulatory molecules and production of cytokines in macrophages. Infect. Immun. **191:**127–137.
27. **Mukherjee, J., G. Nussbaum, M. D. Scharff, and A. Casadevall.** 1995. Protective and nonprotective monoclonal antibodies to *Cryptococcus neoformans* originating from one B cell. J. Exp. Med. **181:**405–409.

28. **Mukherjee, J., M. D. Scharff, and A. Casadevall.** 1992. Protective murine monoclonal antibodies to *Cryptococcus neoformans*. Infect. Immun. **60:**4534–4541.
29. **Mukherjee, S., S. C. Lee, and A. Casadevall.** 1995. Antibodies to *Cryptococcus neoformans* glucuronoxylomannan enhance antifungal activity of murine macrophages. Infect. Immun. **63:**573–579.
30. **Nivens, D. E., D. E. Ohman, J. Williams, and M. J. Franklin.** 2001. Role of alginate and its O acetylation in formation of *Pseudomonas aeruginosa* microcolonies and biofilms. J. Bacteriol. **183:**1047–1057.
31. **Nussbaum, G., W. Cleare, A. Casadevall, M. D. Scharff, and P. Valadon.** 1997. Epitope location in the *Cryptococcus neoformans* capsule is a determinant of antibody efficacy. J. Exp. Med. **185:**685–694.
32. **Nyhus, K. J., A. T. Wilborn, and E. S. Jacobson.** 1997. Ferric iron reduction by *Cryptococcus neoformans*. Infect. Immun. **65:**434–438.
33. **Rosenberg, M., E. A. Bayer, J. Delarea, and E. Rosenberg.** 1982. Role of thin fimbriae in adherence and growth of *Acinetobacter calcoaceticus* RAG-1 on hexadecane. Appl. Environ. Microbiol. **44:**929–937.
34. **Rothstein, T., and M. L. Gefter.** 1983. Affinity analysis of idiotype-positive and idiotype-negative Ars-binding hybridoma proteins and Ars-immune sera. Mol. Immunol. **20:**161–168.
35. **Schembri, M. A., D. Dalsgaard, and P. Klemm.** 2004. Capsule shields the function of short bacterial adhesins. J. Bacteriol. **186:**1249–1257.
36. **Singh, P. K., M. R. Parsek, E. P. Greenberg, and M. J. Welsh.** 2002. A component of innate immunity prevents bacterial biofilm development. Nature **417:**552–555.
37. **Spitzer, E. D., S. G. Spitzer, L. F. Freundlich, and A. Casadevall.** 1993. Persistence of initial infection in recurrent *Cryptococcus neoformans* meningitis. Lancet **341:**595–596.
38. **Syme, R. M., T. F. Bruno, T. R. Kozel, and C. H. Mody.** 1999. The capsule of *Cryptococcus neoformans* reduces T-lymphocyte proliferation by reducing phagocytosis, which can be restored with anticapsular antibody. Infect. Immun. **67:**4620–4627.
39. **Todaro-Luck, F., E. Reiss, R. Cherniak, and L. Kaufman.** 1989. Characterization of *Cryptococcus neoformans* capsular glucuronoxylomannan polysaccharide with monoclonal antibodies. Infect. Immun. **57:**3882–3887.
40. **Vecchiarelli, A.** 2000. Immunoregulation by capsular components of *Cryptococcus neoformans*. Med. Mycol. **38:**407–417.
41. **Walsh, T. J., R. Schlegel, M. M. Moody, J. W. Costerton, and M. Salcman.** 1986. Ventriculoatrial shunt infection due to *Cryptococcus neoformans*: an ultrastructural and quantitative microbiological study. Neurosurgery **18:**373–375.

Editor: T. R. Kozel